Journal of Hydrology 578 (2019) 124115

Contents lists available at ScienceDirect

Journal of Hydrology

journal homepage: www.elsevier.com/locate/jhydrol

Research papers

Forecasting river water temperature time series using a wavelet–neural network hybrid modelling approach

Renata Graf[a], Senlin Zhu[b,*], Bellie Sivakumar[c]

[a] Department of Hydrology and Water Management, Institute of Physical Geography and Environmental Planning, Adam Mickiewicz University in Poznan, Bogumiła Krygowskiego 10 str, 61-680 Poznan, Poland
[b] Department of Civil and Environmental Engineering, Cullen College of Engineering, University of Houston, Houston 77204, USA
[c] Department of Civil Engineering, Indian Institute of Technology Bombay, Powai, Mumbai, Maharashtra 400076, India

ARTICLE INFO

This manuscript was handled by Geoff Syme, Editor-in-Chief

Keywords:
Water temperature forecasting
Wavelet transform
Artificial neural networks
Regression model
Warta River

ABSTRACT

Accurate and reliable water temperature forecasting models can help in environmental impact assessment as well as in effective fisheries management in river systems. In this paper, a hybrid model that couples discrete wavelet transforms (WT) and artificial neural networks (ANN) is proposed for forecasting water temperature. Four mother wavelets, including Daubechies, Symlet, discrete Meyer and Haar, are considered to develop the WT-ANN hybrid model. The hybrid model is applied to forecast daily water temperature on the Warta River in Poland. Time series of daily water temperatures in eight river gauges as well as daily air temperatures of seven meteorological stations are used for forecasting daily water temperature. The performance of this WT-ANN hybrid model is evaluated by comparing the results with those obtained from linear and non-linear regression models as well as a traditional ANN model. The results show that the WT-ANN models perform well in simulating and forecasting river water temperature time series, and outperform the linear, non-linear and traditional ANN models. The superior performance of the WT-ANN models is particularly observed for extreme weather conditions, such as heat waves and drought. Among the four mother wavelets applied, the discrete Meyer performs the best, slightly better than the Daubechies at level 10 and Symlet, while the Haar mother wavelet has the lowest accuracy. In addition, the model performance improves with an increase in the decomposition level, indicating the importance of the choice of decomposition level. The outcomes of this study have important implications for water temperature forecasting and ecosystem management of rivers.

1. Introduction

The temperature of water in rivers is a good indicator of climate variability and change as well as an indicator of the control of processes occurring in river ecosystems and their services (Webb et al., 2008; Letcher et al., 2016). It is an important abiotic factor that shapes optimal conditions for the existence and growth of organisms and preserves the ecological function of the watercourses (Caissie, 2006; Padilla et al., 2015; Letcher et al., 2016). Analysis of the thermal regime of rivers in various climatic and environmental conditions constitutes key information for the assessment of the ecological status of waters.

The temperature of water in rivers is shaped by the influence of the natural environment, undergoing daily, seasonal, annual and decadal changes. Changes in water temperature are mainly in terms of surface heat exchange with the atmosphere, as well as turbulent mixing of water of different temperatures (Caissie, 2006). Accurate and reliable water temperature forecasting models can help in environmental impact assessments as well as in effective fisheries management in river systems.

Many studies on the relationships between water temperature and air temperature have been carried out for the evaluation of long-term trends of their changes and the possibility of their predictions (Mohseni et al., 1998; Mohseni and Stefan, 1999; Webb et al., 2003; Morrill et al., 2005; Webb and Nobilis, 2007; van Vliet et al., 2011; Grbić et al., 2013; Johnson et al., 2014; Nury et al., 2017; Graf, 2018; Zhu et al., 2018, 2019a,b). Such studies have applied simple linear and non-linear regression models and more complex parametric and nonparametric methods (St-Hilaire et al., 2012; Detenbeck et al., 2016). Interesting examples are: the Gaussian process regression models, which are non-parametric kernel-based probabilistic models (Grbić et al., 2013; Zhu et al., 2018) and the cross-correlation function or Granger's causality (Graf, 2018). A majority of such studies have also reported high

* Corresponding author.
E-mail address: szhu20@central.uh.edu (S. Zhu).

https://doi.org/10.1016/j.jhydrol.2019.124115
Received 19 June 2019; Received in revised form 27 August 2019; Accepted 4 September 2019
Available online 05 September 2019

coefficients of determination (> 0.8), demonstrating high dependence of water temperature on air temperature (Pilgrim et al., 1998; Caissie et al., 2001; Webb et al., 2003; Morrill et al., 2005). The traditional statistical/time series methods, such as linear and non-linear regression models, are simple to implement; however, they produce, in general, large modelling errors (van Vliet et al., 2011). On the other hand, the process-based deterministic models are accurate; however, they are often complex and need a lot of information as model inputs, such as river bathymetry, a complete set of meteorological information (air temperature, solar radiation, wind, etc.), inflow and outflow conditions, etc. As a result, application of such models for regions with limited data is impractical.

During the past two decades or so, artificial neural networks (ANN) have been gaining wider applications in forecasting time series, including geophysical, meteorological and hydrological time series. Most ANN applications are used for forecasting in situations where there is an unknown relationship between the set of input factors and the outputs. The ANN model has become a valuable tool for modeling non-linear hydrometeorological phenomena, such as precipitation forecasting (Kuligowski and Barros, 1998; Tokar and Markus, 2000; Ramírez et al., 2005; Chiang et al., 2007; Aksoy and Dahamsheh, 2009; Mandal and Jothiprakash, 2012), streamflow forecasting (Hsu et al., 1995; Sivakumar et al., 2002; Noori and Kalin, 2016; Shiau and Hsu, 2016; Prasad et al., 2017), ground water level simulation (Coulibaly et al., 2001; Lallahem et al., 2005; Daliakopoulos et al., 2005; Nayak et al., 2006; Mohanty et al., 2015; Chang et al., 2015), as well as river water temperature forecasting (Hadzima-Nyarko et al., 2014; Piotrowski et al., 2015; Zhu et al., 2018, 2019a,b; Piotrowski and Napiorkowski, 2019).

Despite their merits and usefulness, applications of the linear and non-linear regression models as well as the traditional ANN models for river water temperature modeling frequently have limitations, especially in processing of non-stationary data, which most hydrological time series are (Tiwari and Chatterjee, 2010; Adamowski and Chan, 2011). In this regard, wavelet transform, as a good pre-processing method for non-stationary data, can be a potential complement for the traditional methods.

Wavelet transform (WT) has been widely used to reveal information (signal) both over time and on a domain scale (frequency). It spreads the main time series into subcomponents, which improves the decomposition of data used in forecasts, and thus enables the capture of useful information at different levels of data resolution. It is particularly useful during data and function analysis, highlighting characteristic points and discontinuities of the input signal. It has been extensively applied in hydrology, such as rainfall–runoff relations for karstic springs (Labat et al., 2001, 2005), scale-dependent synthetic streamflow generation (Niu and Sivakumar, 2013), temporal patterns of precipitation (Niu, 2013; Roushangar et al., 2018), variabilities of hydrological processes (Niu and Chen, 2016; Sang et al., 2018), and hydrological forecasting and regionalization (Maheswaran and Khosa, 2012; Agarwal et al., 2016).

With the ability of ANNs and WT to perform different functions on time series, many studies have developed hybrid WT-ANN models and applied such for forecasting time series in different fields. Such hybrid WT-ANN models have been shown to provide good performance in hydrological studies, such as rainfall-runoff modelling (Shoaib et al., 2016, 2019), streamflow forecasting (Kasiviswanathan et al., 2016; Partal, 2016; Peng et al., 2017; Yaseen et al., 2018), and river water and groundwater level forecasting (Adamowski and Chan, 2011; Seo et al., 2015; Barzegar et al., 2017; Ebrahimi and Rajaee, 2017), among others. Several studies have also shown that the WT-ANN hybrid models perform better than some other widely used models. For example, Peng et al. (2017) applied empirical wavelet transform and artificial neural networks for streamflow forecasting, and reported that the hybrid model can capture the nonlinear characteristics of the streamflow time series and, thus, provide more accurate forecasts than the traditional ANN model. Adamowski and Chan (2011) applied the WT-ANN model to predict groundwater level and stated that the WT-ANN model provided better forecasting accuracy than the conventional ANN model. Similar results have also been reported by Rajaee et al. (2011) and Seo et al. (2016). These studies indicate that the WT-ANN hybrid models allow users to achieve forecasts with higher accuracies.

Despite the fact that the WT-ANN models have found widespread applications in hydrology, their applications for forecasting river water temperature (RWT) have been very limited. To our knowledge, the studies of Piotrowski et al. (2015) and Zhu et al. (2019b) have been the only two, thus far, to apply the hybrid WT-ANN models for RWT prediction. The study of Piotrowski et al. (2015) mainly focused on comparing various artificial neural network types for RWT simulation, including multi-layer perceptron, product-units, adaptive-network-based fuzzy inference systems and WT-ANN. Zhu et al. (2019b) applied the WT-ANN models for RWT forecasting in the Drava River, Croatia. They used the Daubechies at level 10 wavelet. The results showed that the combination of WT and ANN yields better models than the conventional forecasting models for RWT simulation. Since there are many mother wavelets within WT, the choice of the most applicable one is of great importance to accurately forecast RWT. This provided the motivation for the present study.

In this paper, a hybrid model based on coupling discrete WT and ANN for daily river water temperature forecasting was proposed. Compared with previous studies, four widely used mother wavelets were evaluated, for the first time, for RWT forecasting: Daubechies (Db), Symlet (Sym), discrete Meyer (dMey) and Haar. One of the most widely used ANN type, namely the multilayer perceptron neural network (MLPNN), was used here. Eight river gauges in the Warta River in Poland were studied with observation series covering a period of 22 to 27 years. The performance of the hybrid model (WT-ANN) was evaluated by comparing the results with those obtained from linear and non-linear regression models, as well as a traditional ANN model.

2. Methodology

2.1. Linear and non-linear regression models

2.1.1. Linear regression model

For linear regression models, where one dependent variable exists, water temperature is modelled with linear functions. Linear regression models provide a first order estimation of the sensitivity of water temperature to air temperature (Zhu et al., 2018). This simple model is represented as:

$$T_w(t) = A + B \cdot T_a + \varepsilon(t) \quad (1)$$

where $T_w(t)$ is water temperature for a given day t, A and B are regression parameters, and $\varepsilon(t)$ is an error term. T_a is the smoothed air temperature, which can be obtained by the air temperatures from the recent several days, as follows:

$$T_a = \sum_{i=0}^{n} T_a(t-i) \cdot \lambda_i \quad (2)$$

where λ_0 to λ_n are the regression parameters. In the present study, air temperatures over the recent seven days were used.

2.1.2. Non-linear regression model

Mohseni et al. (1998) found a non-linear relationship between water and air temperature. They developed a non-linear regression model for water temperature forecasting based on a logistic S-shaped function. The non-linear regression model proposed by Mohseni et al. (1998) is given as:

$$T_w(t) = \mu + \frac{\alpha - \mu}{1 + e^{\gamma \cdot (\beta - T_a)}} \quad (3)$$

where α is a coefficient which estimates the maximum water temperature, μ is a coefficient which estimates the minimum water

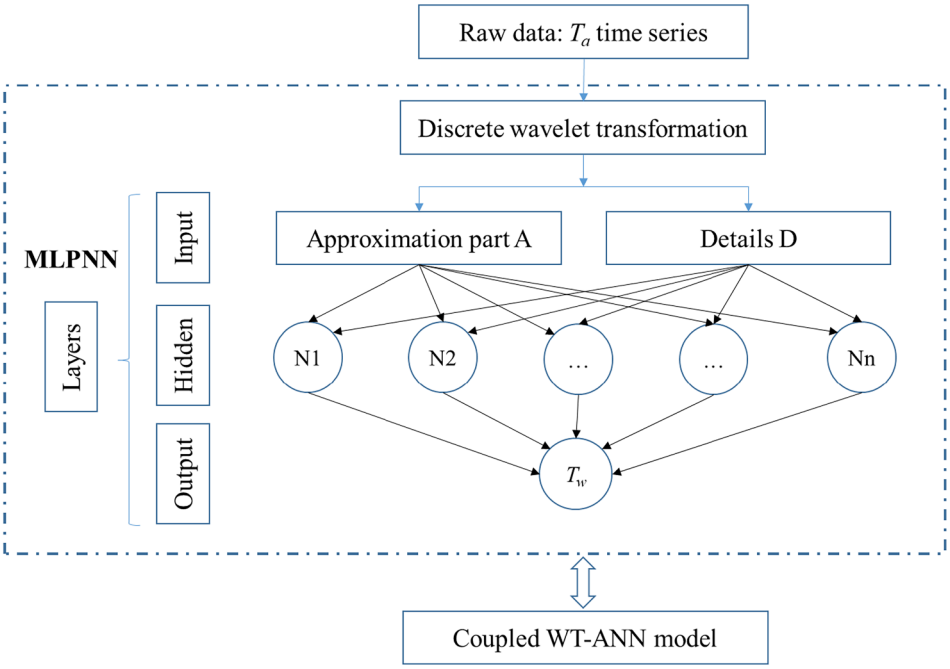

Fig. 1. Flow diagram showing the steps of the combined wavelet transform (WT) and artificial neural network (ANN): T_a is air temperature, WT-ANN is the model coupling of WT and ANN, N1, N2 to Nn are hidden neurons, MLPNN is multilayer perceptron neural network.

temperature, β represents the air temperature at the inflexion point, and γ represents the steepest slope of the logistic S-shaped function.

2.2. Multilayer perceptron neural network (MLPNN)

Artificial neural network models were inspired from the function of human brain, and they have been widely used in various fields. A neural network can be used to forecast future values based on past history. The objective of developing an ANN model is to transform the inputs into meaningful outputs.

The MLPNN is one of the most widely used ANN types. The MLPNN model consists of an input layer, a single hidden layer and one output layer (Fig. 1). The input signal are transmitted through the network in a forward direction and layer by layer. The connections between neurons in different layers are supplied by adjusted weighting values. Each neuron is connected only with neurons in the subsequent layers, and each neuron sums its inputs and later produces its output using a non-linear activation function. The goal of an MLPNN model is to develop a relationship of the form:

$$Y^m = f(X^n) \tag{4}$$

where X^n is model input (including variables x_1, $x_2 \ldots x_n$) and Y^m is model output (including variables y_1, $y_2 \ldots y_m$). For RWT forecasting in this study, x_i is air temperature, and y_i is RWT.

In the MLPNN model used in this study, the observed data were divided into three sets, namely a training dataset, a validation dataset, and a testing dataset. A trial-and-error method was used to determine the optimum number of neurons in the hidden layer. The Levenberg–Marquardt algorithm was used to train the MLPNN models because it is accurate and reliable (Adeloye and De Munari, 2006; Adamowski and Chan, 2011). In the model calibration period, the mean squared error was used to define the network error. For each MLPNN model, we repeated every calibration 30 times, and used the mean squared error as the performance index. To prevent overfitting, early stopping method was used for each model, as suggested by Piotrowski and Napiorkowski (2013). One of the simplest methods of early stopping, namely the Generalization Loss class (Prechlet, 1998; Rowinski and Piotrowski, 2008; Piotrowski and Napiorkowski, 2011), was used, which can help to terminate the training process when validation error exceeds its previously defined minimum value by 20%. Then, the previously defined solution with the lowest objective function value for validation data set was considered as the optimal one.

In the present study, the traditional MLPNN models used the original time series data of air temperature (without transformation by WT) as the model input. To consider the time lags between air temperature and water temperature, air temperature of the recent seven days were used as input.

Data normalization is an important step for MLPNN models. In this study, all the variables were normalized to have zero mean and unit variance using the Z-score method (Olden et al., 2004; Zhu et al., 2019a):

$$x_{ni,k} = \frac{x_{i,k} - m_k}{S_{dk}} \tag{5}$$

where $x_{ni,k}$ is the normalized value of the variable k (input or output) for each sample i, $x_{i,k}$ is the original value of the variable k, and m_k and S_{dk} are the mean value and standard deviation of the variable k.

2.3. Coupled wavelet transform and artificial neural networks (WT–ANN) model

Fig. 1 presents the flow diagram of the steps involved in the combined WT-ANN model. As mentioned earlier, the MLPNN was selected in this study to represent the ANN model. The combination of WT and MLPNN was named WTMLPNN (Fig. 1). The raw time series of daily average air temperatures were firstly transformed into approximation part (A) and several details (D) by WT as pre-processing (see below for further details about WT). Then, the transformed forms of the raw time series of daily average air temperatures were fed into the ANN model as model inputs.

Wavelet transform has been widely applied for the analysis and de-noising of signals and images. Wavelet transform deals with the expansion of functions based on the basis functions. Different from the classical Fourier analysis, WT expands functions in terms of wavelets rather than trigonometric polynomials, which are produced with the form of translations and dilations using a fixed function, namely the

mother wavelet. The raw time series is decomposed by the wavelet transformation into 'wavelets', a scaled and shifted version of the mother wavelet (Robertson et al., 1996; Chaari et al., 1996). Compared with the Fourier Transform (FT), WT has the advantage of simultaneously obtaining information on the time, location and frequency of a signal, while the FT can only provide the frequency information of a signal (Daubechies, 1990). The WT can be divided into two categories: the continuous wavelet transform (CWT) and the discrete wavelet transform (DWT). Compared with the classical CWT, which requires a significant amount of computational time and data, DWT needs less time and is easier to implement (Adamowski and Chan, 2011; Demirel and Anbarjafari, 2011; Nayak et al., 2016).

In this study, the DWT was employed to decompose the original time series data of daily average air temperatures. In the DWT, digital filtering techniques are used to obtain a time-scale signal. The original time series is passed through high-pass and low-pass filters, and detailed coefficients and approximation series are obtained with the wavelet algorithm (Gurley and Kareem, 1999).

Choices of the appropriate mother wavelet and the decomposition level are the two main issues in the applications of DWT (Sun and Chang, 2002; Tascikaraoglu et al., 2016). There are several types of mother wavelets. In this study, we used and compared four widely used mother wavelets: Daubechies (Db), Symlet (Sym), discrete Meyer (dMey) and Haar. These wavelets have been frequently employed in the literature (Nourani et al., 2009, 2011; Chouakri et al., 2011; Adamowski and Chan, 2011; Seo et al., 2015). As for Db in particular, the Daubechies at level 10 (Db10) wavelet has been widely used in the literature, since its wavelet coefficients can capture the maximum amount of signal energy (Chouakri et al., 2011; Seo et al., 2015), and was therefore used in this study as well.

The decomposition level can be determined using the method provided by Nourani et al. (2009). The method has also been applied in Adamowski and Chan (2011) and Seo et al. (2015, 2016) for water level and river stage forecasting. This $\log_{10}$ based method determines the decomposition level using the length of time series data, and is given by:

$$L = int\,[log(P)] \tag{6}$$

where L is the number of decomposition levels, and P is the number of time series data.

To investigate the impact of the decomposition level on modeling performance, we compared wavelets with different decomposition levels.

In this study, the four mother wavelets Db10, Haar, Sym, and dMey were used separately to decompose the original time series of daily air temperatures, and the obtained approximation part (A) and several details (D) were fed into the MLPNN model as forecasters for RWT, respectively. The output results of the four mother wavelets Db10, Haar, Sym, and dMey coupled with MLPNN were named as WTMLPNN1, WTMLPNN2, WTMLPNN3 and WTMLPNN4 respectively. The WTMLPNN models were calibrated by the same algorithm (Levenberg-Marquardt algorithm) as the traditional MLPNN models and used early stopping to avoid over-fitting. For each WTMLPNN model, we repeated every calibration 30 times, and used the mean squared error as the performance index.

2.4. Performance indices

In this study, model performance was evaluated using three indices: the coefficient of determination (R^2), the root mean squared error (*RMSE*), and the mean absolute error (*MAE*). These three indices have been widely used in the literature to assess modeling performance (Morrill et al., 2005; Singh et al., 2009; Adamowski and Chan, 2011).

The R^2 measures the degree of correlation between the observed and modelled values, and is given by:

$$R^2 = \left[\frac{\frac{1}{N}\sum (O_i - O_m)(M_i - M_m)}{\sqrt{\frac{1}{N}\sum_{i=1}^{N}(O_i - O_m)^2}\sqrt{\frac{1}{N}\sum_{i=1}^{N}(M_i - M_m)^2}}\right]^2 \tag{7}$$

where N is the number of samples, O_i is the observed water temperature and M_i is the predicted water temperature at time i, O_m and M_m are the average values of O_i and M_i. The R^2 values range from 0.0 to 1.0, with 1.0 indicating a perfect fit between the modelled values and the observed data.

The *RMSE* indicates the discrepancy between the observed and modelled values, and is given by:

$$RMSE = \sqrt{\frac{1}{N}\sum_{i=1}^{N}(O_i - M_i)^2} \tag{8}$$

A perfect fit would have an *RMSE* value of 0.0.

The *MAE* measures the mean of all the individual errors, and is given by:

$$MAE = \frac{1}{N}\sum_{i=1}^{N}|M_i - O_i| \tag{9}$$

3. Study area and data sources

3.1. Study area

The Warta River in Poland is 808.2 km long and is the largest tributary of the River Oder, which flows into the Baltic Sea (Fig. 2). The Warta River basin covers an area of 5.45×10^4 km^2, which is about 17.4% the entire area of Poland. The main tributaries are: Noteć, Prosna, Ner and Obra. A majority of the region is lowland areas. The northern part of the basin is dominated by low-glacial lowland landscapes, whereas in the southern part, periglacial plains prevails. In the north-western part of the basin, there are extensive forest complexes, separated by agricultural areas, while the middle part is typically agricultural with a small share of forests. Urban areas are also important components of the landscape, with the largest urban areas being Poznań, Łódź and Częstochowa. The Warta River in the area of Uniejów and Poznań stations (see Fig. 2) is under the strong influence of anthropopressure. In Uniejów, the temperature of river waters is influenced by the operation of the Jeziorsko dam reservoir. In Poznań, a high urbanization index is registered, which is manifested, among others, in increased pollution of river waters through uncontrolled inflow of sewage and sewage waters.

The Warta River basin has a typical feature of the transitional climate, with a significant share of oceanic climate features: lower temperature amplitudes, early spring and summer, and relatively short winter. In the northern and northwestern parts, the impact of the maritime climate, resulting from the impact of the Baltic Sea (more cloudy, lower air temperature amplitudes, and cooler summer), is increasingly visible. In the eastern part of the basin, the share of continental climate features (higher amplitudes of air temperature, longer and colder winter) increases.

The average annual air temperature in the region ranges from about 8.3 °C in the northeast to around 8.8 °C in the south and south-west. Poznań is one of the warmest places in this area, and the entire region is one of the warmest in Poland in terms of average annual air temperature. The hottest month is July, and the coldest is January. The average monthly temperature in the region is below zero only in January and February (from 0.0 to −1.0 °C). The summer months are characterized by a smaller range of temperature, and July's average temperature can range from 15.0 °C to over 23.5 °C. The Warta River region, like the whole of Poland, belongs to the regions where the last four decades have seen an increase in temperature in all seasons (Owczarek and Filipiak, 2016).

Fig. 2. Map showing the Warta River and the locations of the water gauges and meteorological stations.

3.2. Data

Daily monitoring of the Warta River water temperature is conducted by the Institute of Meteorology and Water Management - National Research Institute (IMGW-PIB, Warsaw, Poland) with eight river gauges across the region: Bobry, Sieradz and Uniejów (located in the upper course), Nowa Wieś Podgórna, Śrem and Poznań (middle course) and Skwierzyna and Gorzów Wielkopolski (lower course) (Fig. 2). In the vicinity of the water gauge stations, the IMGW-PIB meteorological stations are located, where the daily air temperatures are recorded. Data from these featured river gauges and meteorological stations were analyzed in this study. The data considered cover a period of 22 to 27 hydrological years (hydrological year in Poland is November 1 to October 31). For each river gauge, data sets were divided chronologically into training (4/9), validation (2/9) and testing (1/3) parts. The paired river gauges and meteorological stations with training and testing periods are summarized in Table 1. Fig. 3 presents the time series of daily RWT for the eight river gauges. As seen, RWT in the eight gauges generally is in the range of 0.0–25 °C.

4. Results and discussion

4.1. Model performance for the eight study basin stations

All the parameters for the linear and non-linear regression models were fitted using least squares regression in Excel. In the ANN models, the number of neurons in the hidden layer was varied between 10 and 13 for the eight studied gauges.

The performances of the different models in the training, validation and testing periods for the eight stations in the Warta River are summarized in Table 2.

Linear regression model: The linear model showed slight differences

Table 1
Paired river gauges and meteorological stations with training and testing periods.

River gauges	Meteo station	Training period	Validation period	Testing period	Hydrological years
Bobry	Wieluń	1987–1998	1999–2004	2005–2012	26
Sieradz	Sieradz	1987–1998	1999–2004	2005–2013	27
Uniejów	Koło	1987–1992	1993–1998	2000–2009	22
Nowa Wieś Podgórna	Słupca	1991–2000	2001–2006	2007–2013	23
Śrem	Kórnik	1987–1998	1999–2004	2005–2013	27
Poznań	Poznań	1984–1995	1996–2001	2002–2009	26
Skwierzyna	Gorzów Wlkp.	1987–1996	1997–2002	2003–2010	24
Gorzów Wlkp.	Gorzów Wlkp.	1984–1995	1996–2001	2002–2009	26

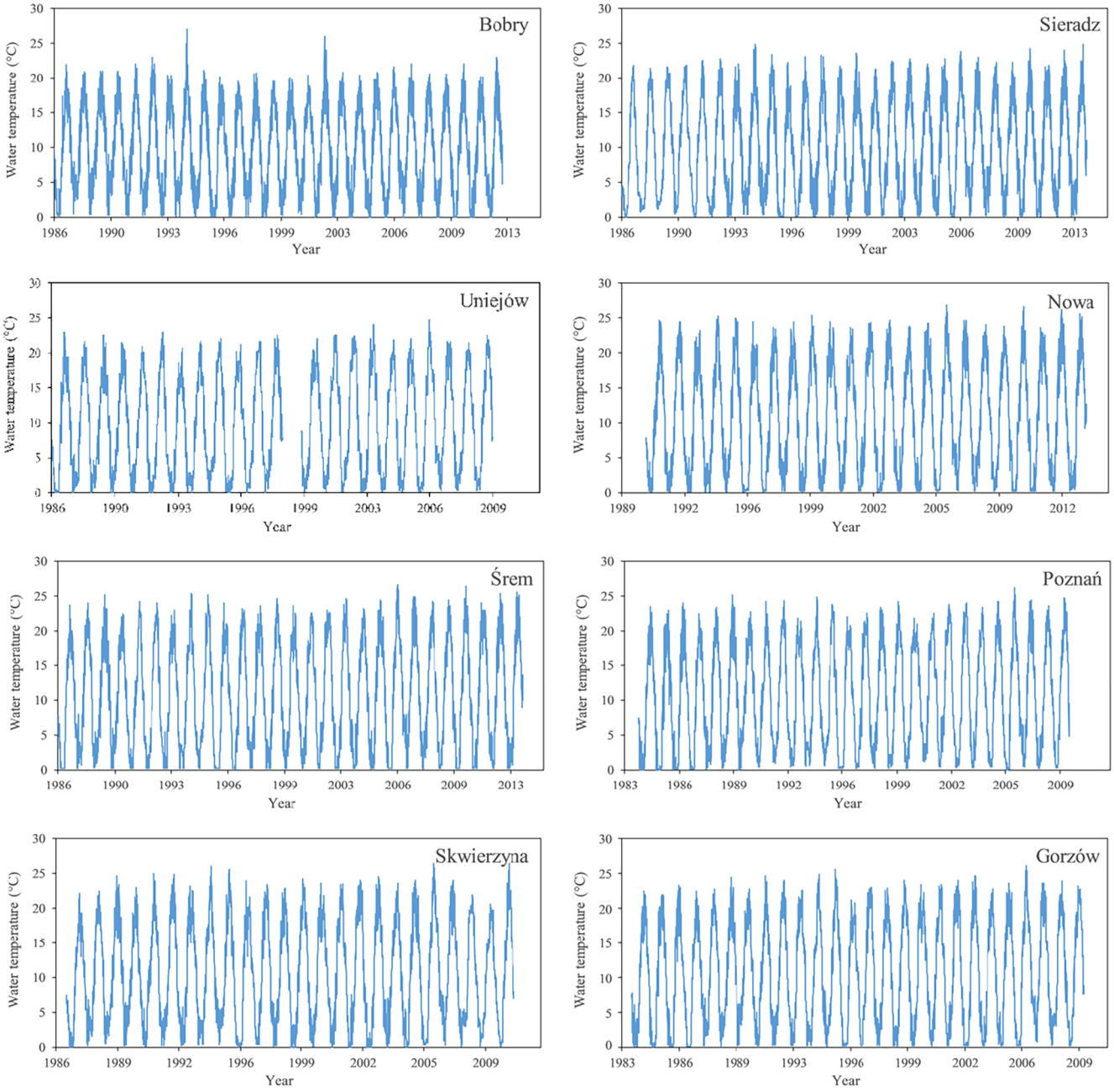

Fig. 3. Time series data of daily water temperatures for the eight river gauges.

in performance for individual river stations in the training, validation and testing periods. The R^2 values ranged from 0.883 (Uniejów) to 0.924 (Sieradz). In the testing periods, higher values of R^2 were obtained, which confirms better performance of the model for this data series, with the exception of Skwierzyna and Nowa Wieś Podgórna stations. These two stations are located at Warta's valleys with low impact of anthropopressure. Fig. 4, for example, presents a comparison of the observed and modelled daily water temperature for the linear (first row) for the testing period at the Bobry station (Fig. 4 also includes such a comparison for the other models used in this study for the Bobry station; see below for details). As seen, the linear regression model yielded many lower water temperature values ($T_w < 0.0\,^{\circ}C$) in the winter period when air temperatures were relatively low (below zero), which is inconsistent with the observed data ($T_w > 0.0\,^{\circ}C$).

Non-linear regression model: The non-linear regression model, based on the logistic S-shaped function, showed greater suitability for forecasting the Warta River water temperature as compared to the linear model. This is evidenced by the higher R^2 values and lower *RMSE* and *MAE* values (Table 2) for the training, validation and testing datasets. For all the eight stations, the nonlinear regression model reproduced the relationship between the air temperature and water temperature ($R^2 = 0.914$–0.957) better than what the linear model did ($R^2 = 0.883$–0.924). The lowest performance by the non-linear model was observed for the Uniejów station (upper river) and the Poznań station (middle river), yielding lower R^2 and higher *RMSE* and *MAE* values ($R^2 = 0.914$–0.920, $RMSE = 1.823$–$2.144\,^{\circ}C$, $MAE = 1.458$–$1.650\,^{\circ}C$). The non-linear model in the testing periods showed an even better performance, which is reflected by the significantly higher R^2 and the decreased values of *RMSE* and *MAE* for most of the gauges. Fig. 4 (second row), for example, presents a comparison of the observed and modelled daily water temperature using the non-linear model for the testing period at the Bobry station. As seen, the matching between the observed and

Table 2
Performances of different models in the training, validation and testing periods (the best models are in bold, and the results are the mean from 30 calibrations).

River station	Model version	Training			Validation			Testing		
		R^2	*RMSE* (°C)	*MAE* (°C)	R^2	*RMSE* (°C)	*MAE* (°C)	R^2	*RMSE* (°C)	*MAE* (°C)
Bobry	Linear	0.893	1.985	1.507	0.894	1.980	1.502	0.908	1.907	1.430
	Non-linear	0.937	1.526	1.169	0.938	1.520	1.162	0.948	1.445	1.140
	MLPNN	0.955	1.370	1.037	0.955	1.322	1.045	0.952	1.400	1.051
	WTMLPNN1	0.963	1.202	0.998	0.963	1.200	0.989	0.964	1.223	0.950
	WTMLPNN2	0.965	1.188	0.982	0.954	1.235	0.980	0.949	1.426	0.980
	WTMLPNN3	0.965	1.194	0.986	0.963	1.210	0.965	0.963	1.228	0.940
	WTMLPNN4	**0.975**	**1.085**	**0.973**	**0.967**	**1.121**	**0.964**	**0.964**	**1.217**	**0.930**
Sieradz	Linear	0.890	2.184	1.682	0.892	2.180	1.678	0.924	1.927	1.420
	Non-linear	0.930	1.753	1.267	0.935	1.746	1.254	0.957	1.459	1.120
	MLPNN	0.955	1.297	1.032	0.959	1.285	0.963	0.969	1.272	0.970
	WTMLPNN1	0.969	1.181	0.982	0.972	1.089	0.952	0.979	1.023	0.890
	WTMLPNN2	0.969	1.197	0.983	0.965	1.223	0.983	0.964	1.245	0.984
	WTMLPNN3	0.971	1.154	0.976	0.973	1.054	0.910	0.981	0.993	0.821
	WTMLPNN4	**0.971**	**1.153**	**0.959**	**0.976**	**1.052**	**0.901**	**0.983**	**0.981**	**0.781**
Uniejów	Linear	0.883	2.442	2.089	0.893	2.437	2.021	0.901	2.150	1.824
	Non-linear	0.914	1.988	1.567	0.915	1.983	1.563	0.920	1.823	1.458
	MLPNN	0.958	1.213	1.028	0.955	1.225	1.056	0.953	1.241	1.086
	WTMLPNN1	0.979	1.018	0.895	0.972	1.121	0.965	0.968	1.211	1.050
	WTMLPNN2	0.976	1.073	0.915	0.964	1.205	1.002	0.953	1.255	1.108
	WTMLPNN3	0.982	1.086	0.908	0.973	1.111	0.952	0.967	1.206	1.069
	WTMLPNN4	**0.988**	**1.033**	**0.887**	**0.982**	**1.056**	**0.943**	**0.978**	**1.110**	**0.959**
Nowa Wieś Podgórna	Linear	0.921	1.894	1.657	0.915	2.150	1.684	0.913	2.318	1.737
	Non-linear	0.952	1.538	1.335	0.950	1.545	1.330	0.950	1.666	1.320
	MLPNN	0.961	1.218	0.983	0.960	1.324	1.121	0.969	1.320	1.041
	WTMLPNN1	0.985	0.857	0.728	0.976	1.125	0.987	0.975	1.301	1.022
	WTMLPNN2	0.983	0.888	0.761	0.974	1.205	0.994	0.967	1.335	1.047
	WTMLPNN3	0.984	0.868	0.747	0.981	1.045	0.965	0.979	1.268	0.984
	WTMLPNN4	**0.985**	**0.849**	**0.726**	**0.983**	**0.993**	**0.894**	**0.983**	**1.080**	**0.930**
Śrem	Linear	0.892	2.501	1.893	0.894	2.480	1.865	0.910	2.364	1.790
	Non-linear	0.923	2.125	1.602	0.928	2.114	1.594	0.944	1.951	1.529
	MLPNN	0.955	1.355	1.017	0.953	1.356	1.023	0.951	1.381	1.046
	WTMLPNN1	0.984	1.114	0.900	0.980	1.156	0.965	0.977	1.227	0.973
	WTMLPNN2	0.978	1.232	0.965	0.962	1.325	0.994	0.956	1.338	1.049
	WTMLPNN3	0.985	1.005	0.885	0.983	1.067	0.913	0.982	1.144	0.933
	WTMLPNN4	**0.985**	**0.987**	**0.796**	**0.985**	**0.992**	**0.856**	**0.987**	**1.008**	**0.893**
Poznań	Linear	0.887	2.460	1.949	0.888	2.500	1.951	0.892	2.505	1.956
	Non-linear	0.920	2.051	1.597	0.917	2.123	1.611	0.918	2.144	1.650
	MLPNN	0.961	1.313	1.144	0.954	1.334	1.211	0.951	1.436	1.290
	WTMLPNN1	0.982	1.133	0.923	0.974	1.204	1.004	0.968	1.303	1.116
	WTMLPNN2	0.977	1.272	1.022	0.968	1.310	1.088	0.962	1.389	1.198
	WTMLPNN3	0.981	1.149	0.961	0.975	1.189	1.026	0.967	1.332	1.212
	WTMLPNN4	**0.982**	**1.132**	**0.903**	**0.978**	**1.134**	**0.978**	**0.974**	**1.262**	**1.032**
Skwierzyna	Linear	0.901	2.016	1.749	0.894	2.230	1.780	0.888	2.503	1.940
	Non-linear	0.929	1.697	1.455	0.918	1.890	1.720	0.915	2.184	1.682
	MLPNN	0.958	1.071	0.975	0.950	1.365	1.245	0.948	1.646	1.473
	WTMLPNN1	0.989	0.908	0.755	0.967	1.312	1.223	0.952	1.523	1.445
	WTMLPNN2	0.986	0.915	0.824	0.964	1.332	1.254	0.952	1.586	1.467
	WTMLPNN3	0.989	0.881	0.754	0.967	1.298	1.203	0.957	1.498	1.348
	WTMLPNN4	**0.989**	**0.868**	**0.734**	**0.972**	**1.178**	**1.067**	**0.966**	**1.434**	**1.286**
Gorzów Wielkopolski	Linear	0.889	2.447	1.973	0.890	2.445	1.975	0.895	2.454	1.980
	Non-linear	0.921	2.080	1.576	0.921	2.071	1.580	0.922	2.131	1.636
	MLPNN	0.954	1.342	1.134	0.950	1.367	1.178	0.947	1.389	1.250
	WTMLPNN1	0.984	1.074	0.853	0.980	1.089	0.945	0.979	1.167	0.982
	WTMLPNN2	0.980	1.166	0.880	0.972	1.224	1.035	0.967	1.337	1.209
	WTMLPNN3	0.984	1.070	0.850	0.974	1.212	1.023	0.970	1.298	1.157
	WTMLPNN4	**0.984**	**1.056**	**0.825**	**0.982**	**1.102**	**0.895**	**0.982**	**1.125**	**0.946**

modelled values was better than that obtained with the linear regression model.

MLPNN model: The MLPNN performed better than that of the non-linear and linear regression models for each of the eight river stations. The R^2 values ranged from 0.947 for the Gorzów Wielkopolski station (testing set) to 0.969 for the Sieradz station (testing set) (Table 2). Generally, the modelling results of MLPNN models are acceptable, with the *RMSE* and *MAE* values ranging from 1.241 to 1.646 °C and from 0.970 to 1.473 °C in the testing period, respectively. Fig. 4 (third row) presents a comparison of the observed and modelled daily water temperature for the MLPNN for the testing period at the Bobry station. The matching between the observed and modelled values was slightly better than that obtained using the non-linear regression model and much better than that obtained using the linear regression model.

WT-ANN hybrid models: The hybrid models used in the forecasting of river water temperature time series showed a high similarity in the results for all the eight stations (Table 2). The results were definitely better than those obtained from the other models, including the MLPNN, as clearly shown in Fig. 5 with the boxplots of R^2, *RMSE* and *MAE* (higher R^2 values and lower *RMSE* and *MAE* values). Comparing the hybrid and the traditional models, both in terms of individual matching of observed versus modelled values through time series and

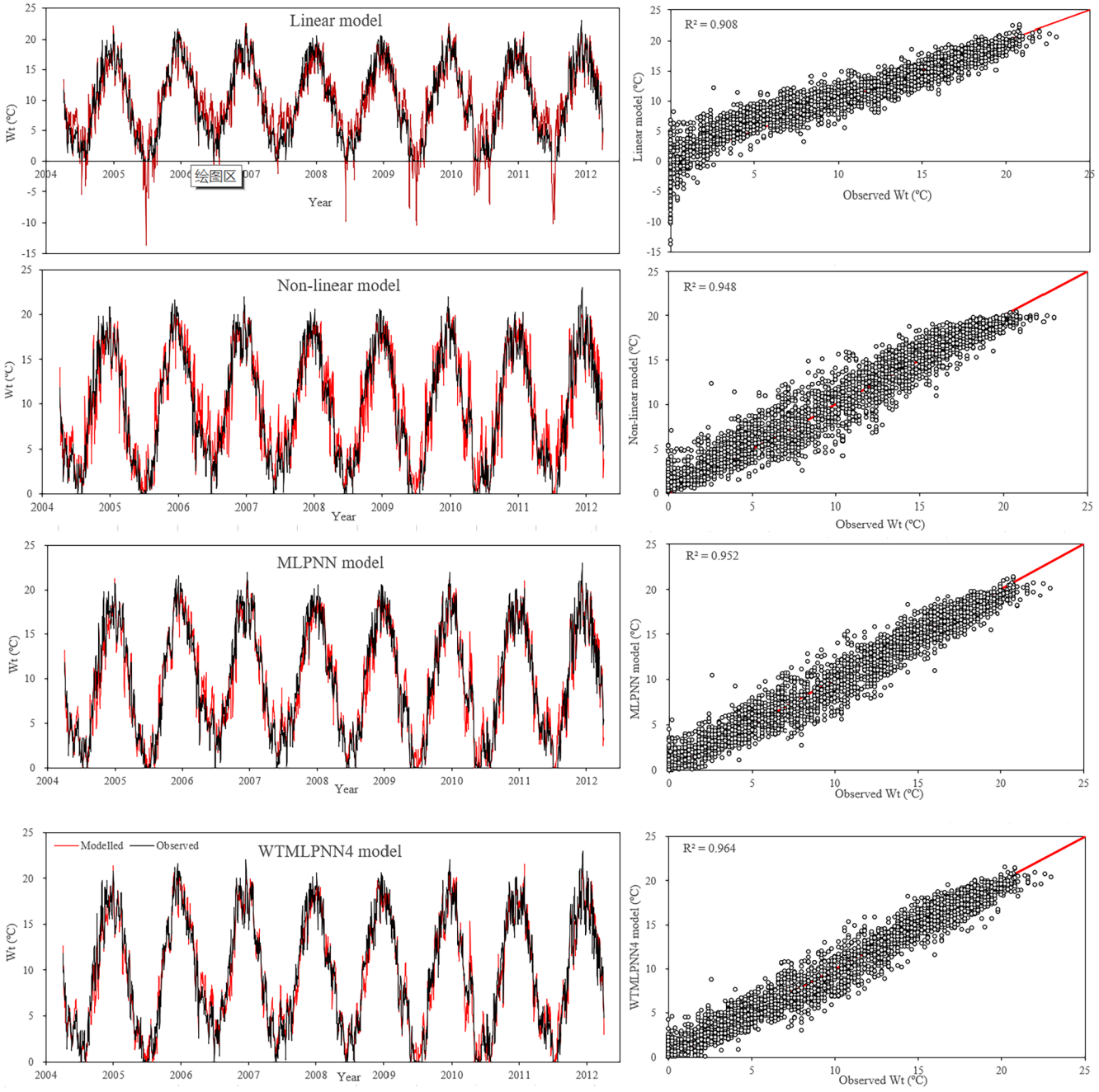

Fig. 4. Comparison of linear, non-linear, MLPNN and WTMLPNN4 models and observed data at the Bobry station for the testing period (Wt: water temperature).

scatter diagrams (Fig. 4) and in terms of the overall performance measures through boxplots of R^2, *RMSE* and *MAE* values (Fig. 5), it can be concluded that the combination of WT and MLPNN yielded more accurate results than the conventional forecasting models used to forecast water temperature in the Warta River. The reason why the WT-MLPNN combination performed better might be that the WT method provided useful decompositions of the original air temperature time series, and the transformed data improved the performance of the MLPNN model by analyzing useful information on various decomposition levels; see Adamowski and Chan (2011) for details. Although the above conclusion for the Warta River cannot be generalized for all rivers and for all situations, the outcomes are nevertheless certainly encouraging on the usefulness and effectiveness of the hybrid WT-ANN models for river water temperature forecasting.

Wavelet transform allows for the transition from a time-value system to a time-scale (frequency) system, which allows analysis of frequency change in the time domain. The present results for the eight stations in the Warta River have shown that the WTMLPNN4 model (with dMey - wavelet decomposition) performed the best (Table 2 and Fig. 5). This model showed slightly better performance compared to the Db wavelet, i.e. Daubechie at level 10 (Db10), whose wavelet coefficients can capture the maximum amount of signal energy (Seo et al., 2015). Compared with other WTMLPNN models, the WTMLPNN2 models have the lowest accuracies, and the modelling results of the WTMLPNN3 models are relatively acceptable (Table 2 and Fig. 5). It is relevant to note, at this point, the study of Nourani et al. (2011) on rainfall-runoff forecasting. Nourani et al. (2011) found that the Haar and Db mother wavelets outperformed Sym. They reasoned that, since runoff time series peaks could be approximated as a single-peaked event with varying durations, the single-peaked wavelets, such as the Haar,

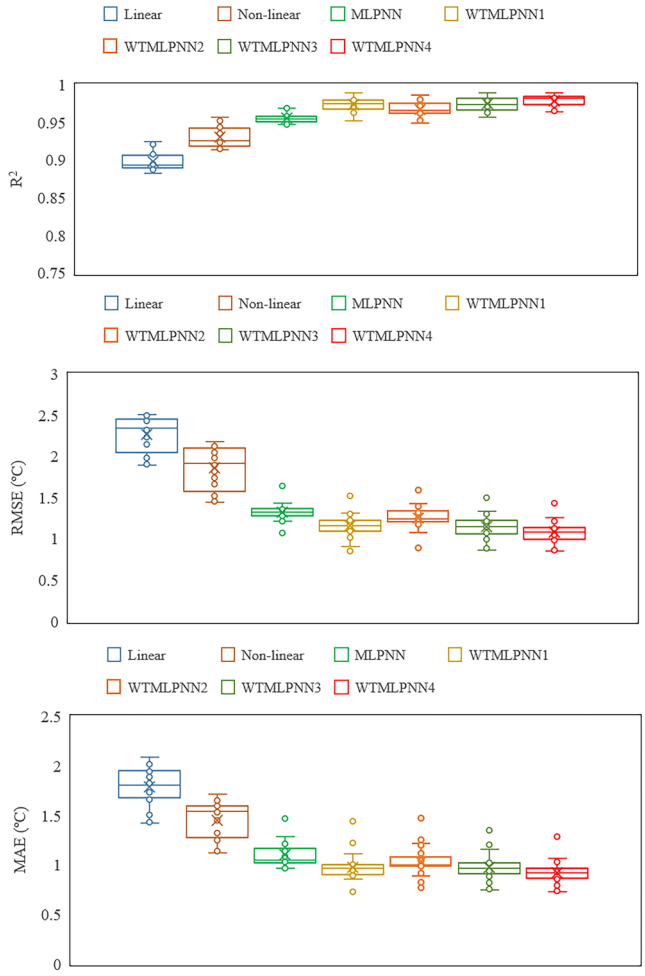

Fig. 5. Boxplots of the R^2, *RMSE* and *MAE* based on all the river stations for all the models during the training, validation and testing periods.

might provide a good estimation of the sharp events contained in the runoff records. However, for RWT forecasting, as is the case in the present study, due to the diurnal variations of air and water temperature, there are usually many peaked values with varying durations. Therefore, the Haar wavelet performed poorly, and the dMey method performed well.

Considering the hybrid models, the best performance was seen for the Sieradz station, for which R^2 in the testing period was in the range of 0.964–0.983, *RMSE* in the range of 0.981–1.245 °C, and *MAE* in the range of 0.781–0.984 °C. Similarly, a high degree of fit was demonstrated by the WTMLPNN models in the case of the Śrem station in the testing period (R^2 = 0.956–0.987, *RMSE* = 1.008–1.338 °C, *MAE* = 0.893–1.049 °C) in the middle region of the Warta River.

To investigate the impact of decomposition level on the performances of the WTMLPNN models (WTMLPNN4), we considered two gauges (Bobry and Sieradz) as examples. In this study, the method of Nourani et al. (2009) was used. This method has also been used, in the past, for water level forecasting and river stage forecasting in Adamowski and Chan (2011) and Seo et al. (2015, 2016), and the results showed that the method is reliable. In the present study, application of this method yielded a decomposition level of 4 for the Bobry and Sieradz stations. However, to confirm this further, we evaluated six decomposition levels for each station (Table 3). For both gauges, model performances improved with an increase in the decomposition level (Table 3), indicating the importance of the choice of the decomposition level. However, improvements in model performances slowed down when the decomposition level was larger than 4. This suggested that using a decomposition level of 4 was enough for the WTMLPNN4 model to obtain considerable accuracy (Table 3). These results further supported the suitability and effectiveness of the method of Nourani et al. (2009). Additionally, a recent study by Quilty and Adamowski (2018) showed that an incorrect development of wavelet-based forecasting models can occur during wavelet decomposition and, as a result, errors can be introduced into the forecast model inputs. One of the main issues in this regard is an inappropriate selection of decomposition levels and wavelet filters (Quilty and Adamowski, 2018), which further indicated the importance of appropriate decomposition levels.

4.2. Model performance during the heat wave and summer drought of 2003 in Europe

In order to properly assess the effectiveness of the models in forecasting water temperature in extreme weather conditions, the model performances were compared for two different periods that had extreme weather conditions across Europe, including Poland: (1) 2000–2005, which corresponded to heat waves across Europe; and (2) the summer drought of 2003.

Fig. 6 (left) presents the time series comparison of the observed and modelled river water temperatures for the period 2000–2005 when the traditional ANN model (MLPNN) and a hybrid model (WTMLPNN4) were used, for three stations: Bobry (upstream) (top panel), Śrem (middle river run) (middle panel), and Gorzów Wielkopolski (downstream) (bottom panel). The figure also includes the air temperature, for a proper perspective on the relationship between air temperature and water temperature. As seen, the modelling results of the MLPNN fluctuate sharply compared with the observed data. However, the WTMLPNN4 model was more stable and accurate for each station, indicating that, with the coupling of WT, the MLPNN model tended to be more robust and could better capture the seasonal thermal dynamics during heat wave events.

The validity of the MLPNN and WTMLPNN4 models for the three river stations was also tested specifically for the heat wave and drought of July and August 2003 (Fig. 6, right). The WTMLPNN4 model well reproduced the observed time series of water temperature, and it clearly outperformed the (traditional) MLPNN model for each station. The results further indicated that, with the coupling of WT, the MLPNN model was able to better capture the thermal dynamics during summer droughts.

5. Conclusions

In this study, a hybrid model (WTMLPNN), by coupling wavelet transform (WT) and multilayer perceptron neural network (MLPNN), was developed to achieve better forecasts for water temperature in rivers. The model was applied to data from eight stations in the Warta River in Poland. Four different WTMLPNN models were considered, based on four different mother wavelets. The performances of these models were compared with linear and non-linear regression models as well as traditional MLPNN models. The results lead to the following conclusions:

(1) The MLPNN models outperformed the linear and non-linear regression models for the eight stations.
(2) The hybrid WTMLPNN models performed much better than the traditional MLPNN model in both normal and heat wave/drought conditions.
(3) The WTMLPNN model with the discrete Meyer (dMEY) mother wavelet performed the best (average R^2 = 0.979, *RMSE* = 1.084 °C, *MAE* = 0.919 °C), slightly better than the Daubechies level 10 (Db10) mother wavelet (average R^2 = 0.974, *RMSE* = 1.157 °C, *MAE* = 0.979 °C) and the Symlet (Sym) (average R^2 = 0.975, *RMSE* = 1.148 °C, *MAE* = 0.979 °C). The WTMLPNN model with the Haar mother wavelet performed the worst (average R^2 = 0.967, *RMSE* = 1.246 °C, *MAE* = 1.029 °C).

Table 3
Impact of decomposition level on performances of WTMLPNN models in the training, validation and testing periods (the results are the mean from 30 calibrations) for the Bobry and Sieradz stations.

River station	Decomposition level	Training			Validation			Testing		
		R^2	*RMSE* (°C)	*MAE* (°C)	R^2	*RMSE* (°C)	*MAE* (°C)	R^2	*RMSE* (°C)	*MAE* (°C)
Bobry	1	0.955	1.344	1.025	0.946	1.324	1.047	0.941	1.376	1.047
	2	0.958	1.230	1.017	0.948	1.315	1.040	0.950	1.325	1.012
	3	0.964	1.153	0.997	0.952	1.213	0.998	0.958	1.285	0.980
	4	0.975	1.085	0.973	0.967	1.121	0.964	0.964	1.217	0.930
	5	0.978	1.082	0.967	0.970	1.112	0.957	0.966	1.215	0.925
	6	0.980	1.080	0.962	0.972	1.087	0.945	0.968	1.212	0.921
Sieradz	1	0.956	1.292	1.030	0.960	1.282	0.960	0.970	1.267	0.967
	2	0.962	1.272	1.014	0.965	1.178	0.945	0.975	1.197	0.904
	3	0.967	1.184	0.989	0.970	1.035	0.924	0.980	1.055	0.845
	4	0.971	1.153	0.959	0.976	1.052	0.901	0.983	0.981	0.781
	5	0.972	1.145	0.954	0.978	1.047	0.896	0.984	0.979	0.778
	6	0.974	1.142	0.950	0.980	1.042	0.893	0.984	0.978	0.776

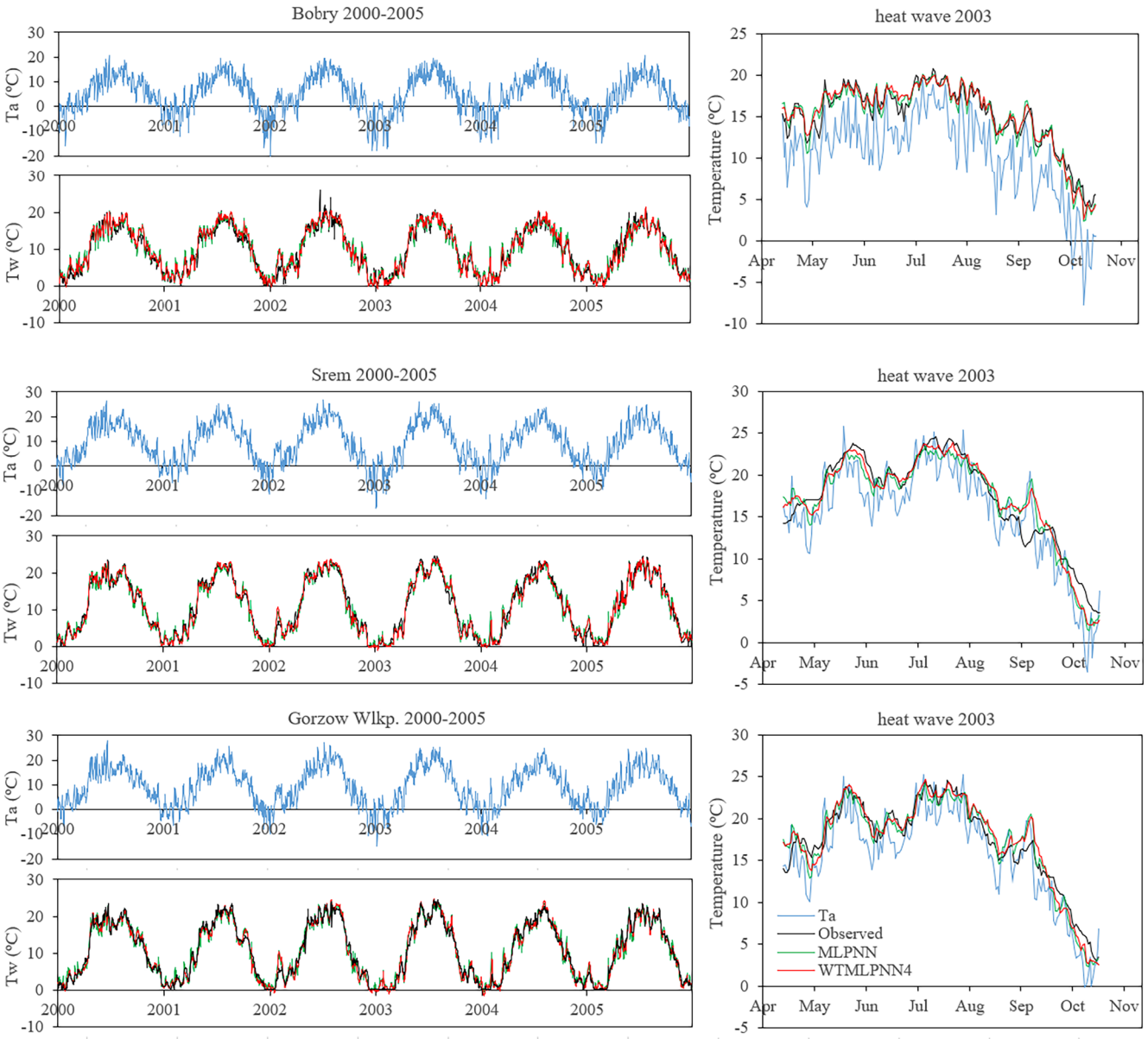

Fig. 6. Observed daily water temperatures and simulated daily water temperatures for the MLPNN and WTMLPNN4 models during the period 2000–2005, and during the heat wave and summer drought of 2003 (Ta: air temperature) at the Bobry (upstream), Śrem (middle river), and Gorzów Wielkopolski (downstream) stations.

(4) Model performances improved with an increase in the decomposition level in the wavelet transform, indicating the importance of the choice of the decomposition level. The results in this study provided further support to the applicability of the method of Nourani et al. (2009) to determine the optimum decomposition level.

The outcomes of the present study have important implications for research on forecasting the temperature of water in rivers, especially from the viewpoint of coupling/integrating wavelets and ANNs in particular, and different time series/data-based methods more broadly. Though the hybrid WTMLPNN models performed well, there is still scope for further improvements through additional studies. Firstly, according to some previous studies, flow discharge may play an important role on river water temperature forecasting, especially in rivers impacted by snow or higher altitude hydropower reservoirs (Piccolroaz et al., 2016; Zhu et al., 2019a). However, due to lack of complete data, flow discharge was not considered in this study. Therefore, in a future study, we will further improve the hybrid models by including flow discharge as a model input for rivers with available flow discharge data. Secondly, there are many other factors that influence river temperature as well (e.g., irradiance, shading, water depth, slope, groundwater inputs), and we have not considered all these factors in this study. Nevertheless, our model showed good predictability in calibration and validation period using long-term observed data, and during model calibration and validation, even when the above factors were not taken into consideration. We intend to look into the other factors in our future research, to further improve the model accuracy. Lastly, though eight river gauges were assessed in the present study, they were all in only one river. Therefore, offering general conclusions on the effectiveness of the hybrid WTMLPNN models and the superiority of such over traditional models for any river around the world is not possible. Our future research will focus on further refining the coupling as well as application of the hybrid models to different rivers around the world to more properly test the suitability and effectiveness of the models for rivers characterized by different climatic, hydrological, and land use regimes.

CRediT authorship contribution statement

Renata Graf: Conceptualization, Methodology, Project administration, Investigation, Software, Formal analysis, Validation, Visualization, Writing - original draft, Writing - review & editing. **Senlin Zhu:** Supervision, Funding acquisition, Project administration, Conceptualization, Writing - review & editing. **Bellie Sivakumar:** Supervision, Writing - review & editing.

Declaration of Competing Interest

The authors declare that they have no known competing financial interests or personal relationships that could have appeared to influence the work reported in this paper.

Acknowledgments

This research was supported by the Office of Science of the U.S. Department of Energy through the Energy Exascale Earth System Modeling (E3SM) project of Earth System Modeling program.

References

Adamowski, J., Chan, H.F., 2011. A wavelet neural network conjunction model for groundwater level forecasting. J. Hydrol. 407, 28–40.
Adeloye, A.J., De Munari, A., 2006. Artificial neural network based generalized storage–yield–reliability models using the Levenberg–Marquardt algorithm. J. Hydrol. 326 (1–4), 215–230.
Agarwal, A., Maheswaran, R., Sehgal, V., Khosa, R., Sivakumar, B., Bernhofer, C., 2016. Hydrologic regionalization using wavelet-based multiscale entropy method. J. Hydrol. 538, 22–32.
Aksoy, H., Dahamsheh, A., 2009. Artificial neural network models for forecasting monthly precipitation in Jordan. Stoch. Env. Res. Risk Assess. 23 (7), 917–931.
Barzegar, R., Fijani, E., Moghaddam, A.A., Tziritis, E., 2017. Forecasting of groundwater level fluctuations using ensemble hybrid multi-wavelet neural network-based models. Sci. Total Environ. 599–600, 20–31.
Caissie, D., 2006. The thermal regime of rivers: a review. Freshw. Biol. 51 (8), 1389–1406.
Caissie, D., El-Jabi, N., Satish, M.G., 2001. Modelling of maximum daily water temperatures in a small stream using air temperatures. J. Hydrol. 251 (1–2), 14–28.
Chaari, O., Meunier, M., Brouaye, F., 1996. Wavelets: a new tool for the resonant grounded power distribution systems relaying. IEEE Trans. Power Deliv. 11 (3), 1301–1308.
Chang, J., Wang, G., Mao, T., 2015. Simulation and prediction of suprapermafrost groundwater level variation in response to climate change using a neural network model. J. Hydrol. 529 (3), 1211–1220.
Chiang, Y., Chang, F., Jou, B.J., Lin, P., 2007. Dynamic ANN for precipitation estimation and forecasting from radar observations. J. Hydrol. 334 (1–2), 250–261.
Chouakri, S.A., Bereksi-Reguigb, F., Taleb-Ahmedc, A., 2011. QRS complex detection based on multi wavelet packet decomposition. Appl. Math. Comput. 217 (23), 9508–9525.
Coulibaly, P., Anctil, F., Aravena, R., Bobée, B., 2001. Artificial neural network modeling of water table depth fluctuations. Water Resour. Res. 37 (4), 885–896.
Daliakopoulos, I.N., Coulibaly, P., Tsanis, I.K., 2005. Groundwater level forecasting using artificial neural networks. J. Hydrol. 309 (1–4), 229–240.
Daubechies, I., 1990. The wavelet transform, time-frequency localization and signal analysis. IEEE Trans. Inf. Theory 36 (5), 961–1005.
Demirel, A., Anbarjafari, G., 2011. Discrete wavelet transform-based satellite image resolution enhancement. IEEE Trans. Geosci. Remote Sens. 49 (6), 1997–2004.
Detenbeck, N.E., Morrison, A.C., Abele, R.W., Kopp, D.A., 2016. Spatial statistical network models for stream and river temperature in New England, USA. Water Resour. Res. 52 (8), 6018–6040.
Ebrahimi, H., Rajaee, T., 2017. Simulation of groundwater level variations using wavelet combined with neural network, linear regression and support vector machine. Global Planet. Change 148, 181–191.
Graf, R., 2018. Distribution properties of a measurement series of river water temperature at different time resolution levels (based on the example of the Lowland River Noteć, Poland). Water 10 (2), 203.
Grbić, R., Kurtagić, D., Slišković, D., 2013. Stream water temperature prediction based on Gaussian process regression. Expert Syst. Appl. 40 (18), 7407–7414.
Gurley, K., Kareem, A., 1999. Applications of wavelet transforms in earthquake, wind and ocean engineering. Eng. Struct. 21, 149–167.
Hadzima-Nyarko, M., Rabi, A., Šperac, M., 2014. Implementation of artificial neural networks in modeling the water-air temperature relationship of the River Drava. Water Resour. Manage. 28 (5), 1379–1394.
Hsu, K.L., Gupta, H.V., Sorooshian, S., 1995. Artificial neural network modeling of the rainfall-runoff process. Water Resour. Res. 31 (10), 2517–2530.
Johnson, M.F., Wilby, R.L., Toone, J.A., 2014. Inferring air–water temperature relationships from river and catchment properties. Hydrol. Process. 28 (6), 2912–2928.
Kasiviswanathan, K.S., He, J., Sudheer, K.P., Tay, J., 2016. Potential application of wavelet neural network ensemble to forecast streamflow for flood management. J. Hydrol. 536, 161–173.
Kuligowski, R.J., Barros, A.P., 1998. Localized precipitation forecasts from a numerical weather prediction model using artificial neural networks. Weather Forecasting 13, 1194–1204.
Labat, D., Ababou, R., Mangin, A., 2001. Introduction of wavelet analyses to rainfall/runoffs relationship for a karstic basin: the case of Licq-Atherey karstic system (France). Groundwater 39 (4), 605–615.
Labat, D., Ababou, R., Mangin, A., 2005. Rainfall–runoff relations for karstic springs. Part II: continuous wavelet and discrete orthogonal multiresolution analyses. J. Hydrol. 238 (3–4), 149–178.
Lallahem, S., Mania, J., Hani, A., Najjar, Y., 2005. On the use of neural networks to evaluate groundwater levels in fractured media. J. Hydrol. 307 (1–4), 92–111.
Letcher, B.H., Hocking, D.J., O'Neil, K., Whiteley, A.R., Nislow, K.H., O'Donnell, M.J., 2016. A hierarchical model of daily stream temperature using air-water temperature synchronization, autocorrelation, and time lags. PeerJ 4, e1727.
Maheswaran, R., Khosa, R., 2012. Comparative study of different wavelets for hydrologic forecasting. Comput. Geosci. 46, 284–295.
Mandal, T., Jothiprakash, V., 2012. Short-term rainfall prediction using ANN and MT techniques. ISH J. Hydraulic Eng. 18 (1), 20–26.
Mohanty, S., Jha, M.K., Raul, S.K., Panda, R.K., Sudheer, K.P., 2015. Using artificial neural wetwork approach for simultaneous forecasting of weekly groundwater levels at multiple sites. Water Resour. Manage. 29 (15), 5521–5532.
Mohseni, O., Stefan, H.G., Erickson, T.R., 1998. A non-linear regression model for weekly stream temperatures. Water Resour. Res. 34, 2685–2692.
Mohseni, O., Stefan, H.G., 1999. Stream temperature/air temperature relationship: a physical interpretation. J. Hydrol. 218 (3–4), 128–141.
Morrill, J.C., Bales, R.C., Conklin, M.H., 2005. Estimating stream temperature from air temperature: implications for future water quality. J. Environ. Eng. 131 (1), 139–146.
Nayak, D.R., Dash, R., Majhi, B., 2016. Brain MR image classification using two-dimensional discrete wavelet transform and AdaBoost with random forests. Neurocomputing 177, 188–197.
Nayak, P.C., Rao, Y.R.S., Sudheer, K.P., 2006. Groundwater level forecasting in a shallow aquifer using artificial neural network approach. Water Resour. Manage. 20 (1), 77–90.
Niu, J., 2013. Precipitation in the Pearl River basin, South China: scaling, regional

patterns, and influence of large-scale climate anomalies. Stoch. Env. Res. Risk Assess. 27 (5), 1253–1268.
Niu, J., Chen, J., 2016. A wavelet perspective on variabilities of hydrological processes in conjunction with geomorphic analysis over the Pearl River basin in South China. J. Hydrol. 542, 392–409.
Niu, J., Sivakumar, B., 2013. Scale-dependent synthetic streamflow generation using a continuous wavelet transform. J. Hydrol. 496, 71–78.
Noori, N., Kalin, L., 2016. Coupling SWAT and ANN models for enhanced daily streamflow prediction. J. Hydrol. 533, 141–151.
Nourani, V., Alami, M., Aminfar, M., 2009. A combined neural-wavelet model for prediction of Ligvanchai watershed precipitation. Eng. Appl. Artif. Intell. 22, 466–472.
Nourani, V., Kisi, Ö., Komasi, M., 2011. Two hybrid Artificial Intelligence approaches for modeling rainfall–runoff process. J. Hydrol. 402, 41–59.
Nury, A.H., Hasan, K., Alam, M.J.B., 2017. Comparative study of wavelet-ARIMA and wavelet-ANN models for temperature time series data in northeastern Bangladesh. J. King Saud Univ. Sci. 29 (1), 47–61.
Olden, J.D., Joy, M.K., Death, R.G., 2004. An accurate comparison of methods for quantifying variable importance in artificial neural networks using simulated data. Ecol. Model. 178, 389–397.
Owczarek, M., Filipiak, J., 2016. Contemporary changes of thermal conditions in Poland, 1951–2015. Bull. Geogr. Phys. Geogr. Ser. 10, 31–50.
Padilla, A., Rasouli, K., Déry, S.J., 2015. Impacts of variability and trends in runoff and water temperature on salmon migration in the Fraser River Basin. Canada 60 (3), 523–533.
Partal, T., 2016. Wavelet regression and wavelet neural network models for forecasting monthly streamflow. J. Water Clim. Change 8 (1), 48–61.
Peng, T., Zhou, J., Zhang, C., Fu, W., 2017. Streamflow forecasting using empirical wavelet transform and artificial neural networks. Water 9 (6), 406.
Piccolroaz, S., Calamita, E., Majone, B., Gallice, A., Siviglia, A., Toffolon, M., 2016. Prediction of river water temperature: a comparison between a new family of hybrid models and statistical approaches. Hydrol. Process. 30, 3901–3917.
Pilgrim, J.M., Fang, X., Stefan, H.Z., 1998. Stream temperature correlations with air temperatures in Minnesota: implications for climate warming. J. Am. Water Resour. Assoc. 34 (5), 1109–1121.
Piotrowski, A.P., Napiorkowski, J.J., 2011. Optimizing neural networks for river flow forecasting – evolutionary computation methods versus the Levenberg–Marquardt approach. J. Hydrol. 407 (1–4), 12–27.
Piotrowski, A.P., Napiorkowski, J.J., 2013. A comparison of methods to avoid overfitting in neural networks training in the case of catchment runoff modelling. J. Hydrol. 476, 97–111.
Piotrowski, A.P., Napiorkowski, M.J., Napiorkowski, J.J., Osuch, M., 2015. Comparing various artificial neural network types for water temperature prediction in rivers. J. Hydrol. 529 (1), 302–315.
Piotrowski, A.P., Napiorkowski, J.J., 2019. Simple modifications of the nonlinear regression stream temperature model for daily data. J. Hydrol. 572, 308–328.
Prasad, R., Deo, R.C., Li, Y., Maraseni, T., 2017. Input selection and performance optimization of ANN-based streamflow forecasts in the drought-prone Murray Darling Basin region using IIS and MODWT algorithm. Atmos. Res. 197, 42–63.
Prechlet, L., 1998. Automatic early stopping using cross-validation: quantifying the criteria. Neural Networks 11 (4), 761–777.
Quilty, J., Adamowski, J., 2018. Addressing the incorrect usage of wavelet-based hydrological and water resources forecasting models for real-world applications with best practices and a new forecasting framework. J. Hydrol. 563, 336–353.
Rajaee, T., Nourani, V., Zounematkermani, M., Kisi, O., 2011. River suspended sediment load prediction: application of ANN and wavelet conjunction model. J. Hydrol. Eng. 16 (8), 613–627.
Ramírez, M.C.V., Velho, H.F.C., Ferreira, N.J., 2005. Artificial neural network technique for rainfall forecasting applied to the São Paulo region. J. Hydrol. 301 (1–4), 146–162.
Robertson, D.C., Camps, O.I., Mayer, J.S., Gish, W.B., 1996. Wavelets and electromagnetic power system transients. IEEE Trans. Power Deliv. 11 (2), 1050–1058.
Roushangar, K., Nourani, V., Alizadeh, F., 2018. A multiscale time-space approach to analyze and categorize the precipitation fluctuation based on the wavelet transform and information theory concept. Hydrol. Res. 49 (3), 724–743.
Rowinski, P.M., Piotrowski, A., 2008. Estimation of parameters of transient storage model by means of multi-layer perceptron neural networks. Hydrol. Sci. J. 53 (1), 165–178.
Sang, Y., Sun, F., Singh, V.P., Xie, P., Sun, J., 2018. A discrete wavelet spectrum approach for identifying non-monotonic trends in hydroclimate data. Hydrol. Earth Syst. Sci. 22, 757–766.
Seo, Y., Kim, S., Kisi, O., Singh, V.P., 2015. Daily water level forecasting using wavelet decomposition and artificial intelligence techniques. J. Hydrol. 520, 224–243.
Seo, Y., Kim, S., Kisi, O., Singh, V.P., Parasuraman, K., 2016. River stage forecasting using wavelet packet decomposition and machine learning models. Water Resour. Manage. 30 (11), 1–25.
Shiau, J., Hsu, H., 2016. Suitability of ANN-based daily streamflow extension models: a case study of Gaoping River Basin, Taiwan. Water Resour. Manage. 30 (4), 1499–1513.
Shoaib, M., Shamseldin, A.Y., Melville, B.W., Khan, M.M., 2016. A comparison between wavelet based static and dynamic neural network approaches for runoff prediction. J. Hydrol. 535, 211–225.
Shoaib, M., Shamseldin, A.Y., Khan, M.M., Sultan, M., Ahmad, F., Sultan, T., Dahri, Z.H., Ali, I., 2019. Input selection of wavelet-coupled neural network models for rainfall-runoff modelling. Water Resour. Manage. 33 (3), 955–973.
Singh, K.P., Basant, A., Malik, A., Jain, G., 2009. Artificial neural network modeling of the river water quality—a case study. Ecol. Model. 220, 888–895.
Sivakumar, B., Jayawardena, A.W., Fernando, T.M.K.G., 2002. River flow forecasting: use of phase-space reconstruction and artificial neural networks approaches. J. Hydrol. 265 (1–4), 225–245.
St-Hilaire, A., Ouarda, T.B.M.J., Bargaoui, Z., Daigle, A., Bilodeau, L., 2012. Daily river water temperature forecast model with a k-nearest neighbour approach. Hydrol. Process. 26 (9), 1302–1310.
Sun, Z., Chang, C.C., 2002. Structural damage assessment based on wavelet packet transform. J. Struct. Eng. 128 (10), 1354–1361.
Tascikaraoglu, A., Sanandaji, B.M., Poolla, K., Varaiya, P., 2016. Exploiting sparsity of interconnections in spatio-temporal wind speed forecasting using Wavelet Transform. Appl. Energy 165, 735–747.
Tiwari, M.K., Chatterjee, C., 2010. Development of an accurate and reliable hourly flood forecasting model using wavelet–bootstrap–ANN (WBANN) hybrid approach. J. Hydrol. 1 (394), 458–470.
Tokar, A.S., Markus, M., 2000. Precipitation-runoff modeling using artificial neural networks and conceptual models. J. Hydrol. Eng. 5 (2), 156–161.
van Vliet, M.T.H., Ludwig, F., Zwolsman, J.J.G., Weedon, G.P., Kabat, P., 2011. Global river temperatures and sensitivity to atmospheric warming and changes in river flow. Water Resour. Res. 47 (2), W02544.
Webb, B.W., Clark, P.D., Walling, D.E., 2003. Water–air temperature relationships in a Devon river system and the role of flow. Hydrol. Process. 17 (15), 3069–3084.
Webb, B.W., Nobilis, F., 2007. Long-term changes in river temperature and the influence of climatic and hydrological factors. Hydrol. Sci. J. 52, 74–85.
Webb, B.W., Hannah, D.M., Moore, R.D., Brown, L.E., Nobilis, F., 2008. Recent advances in stream and river temperature research. Hydrol. Process. 22 (7), 902–918.
Yaseen, Z.M., Fu, M., Wang, C., Mohtar, W.H.M.W., Deo, R.C., El-shafie, A., 2018. Application of the hybrid artificial neural network coupled with rolling mechanism and grey model algorithms for streamflow forecasting over multiple time horizons. Water Resour. Manage. 32 (5), 1883–1899.
Zhu, S., Nyarko, E.K., Hadzima-Nyarko, M., 2018. Modelling daily water temperature from air temperature for the Missouri River. PeerJ 6, e4894.
Zhu, S., Heddam, S., Nyarko, E.K., Hadzima-Nyarko, M., Piccolroaz, S., Wu, S., 2019a. Modeling daily water temperature for rivers: comparison between adaptive neuro-fuzzy inference systems and artificial neural networks models. Environ. Sci. Pollut. Res. 26 (1), 402–420.
Zhu, S., Hadzima-Nyarko, M., Gao, A., Wang, F., Wu, J., Wu, S., 2019b. Two hybrid data-driven models for modeling water-air temperature relationship in rivers. Environ. Sci. Pollut. Res. 26 (12), 12622–12630.